

HSDPA and MBMS Transmissions via S-UMTS

Giovanni Giambene[°], Samuele Giannetti[°], Victor Y. H. Kueh*, Cristina Párraga Niebla[‡]

[°] Dipartimento di Ingegneria dell'Informazione, Università degli Studi di Siena, Via Roma, 56 - 53100
Siena, Italy, Email: giambene@unisi.it, giannetti12@unisi.it

*Centre for Communication Systems Research, University of Surrey, Guildford, Surrey GU2 7XH, UK

[‡]German Aerospace Center (DLR), Institute of Communications and Navigation, Oberpfaffenhofen,
P.O.Box 11 16, D-82230 Wessling, Germany, Email: cristina.parraga@dlr.de

5th MCM of COST 290 Action, Delft, The Netherlands, February 9-10, 2006

Paper code: TD(06)013

Abstract

This paper investigates packet-scheduling aspects for satellite UMTS downlink transmissions in two special cases: *High Speed Downlink Packet Access* (HSDPA) and *Multimedia Broadcast Multicast Services* (MBMS). In particular, this paper surveys resource allocation constraints to be considered for HSDPA via satellite and investigates the applicability of *Adaptive Modulation and Coding* (AMC) in conjunction with packet scheduling. This paper provides considerations that support the adoption of HSDPA and MBMS via satellite and preliminary results for the HSDPA case.

Keywords

Satellite Communications, Geostationary Satellites, S-HSDPA, Traffic Scheduling, Proportional Fairness

HSDPA and MBMS Transmissions via S-UMTS

Giovanni Giambene[°], Samuele Giannetti[°], Victor Y. H. Kueh^{*}, Cristina Párraga[‡]

[°] Dipartimento di Ingegneria dell'Informazione, Università degli Studi di Siena, Via Roma, 56 - 53100
Siena, Italy

^{*}Centre for Communication Systems Research, University of Surrey, Guildford, Surrey GU2 7XH, UK

[‡]German Aerospace Center (DLR), Institute of Communications and Navigation, Oberpfaffenhofen,
P.O.Box 11 16, D-82230 Wessling, Germany

Abstract: This paper investigates packet-scheduling aspects for satellite UMTS downlink transmissions in two special cases: *High Speed Downlink Packet Access (HSDPA)* and *Multimedia Broadcast Multicast Services (MBMS)*. In particular, this paper surveys resource allocation constraints to be considered for HSDPA via satellite and investigates the applicability of *Adaptive Modulation and Coding (AMC)* in conjunction with packet scheduling. This paper provides considerations that support the adoption of HSDPA and MBMS via satellite and preliminary results for the HSDPA case. This work has been carried out within the framework of the "SatNEx" NoE project (contract No. 507052) - joint activity 2430 (QoS&RRM).

1. Introduction

Third-generation terrestrial cellular systems, namely *Universal Mobile Telecommunication System (UMTS)*, envisage a satellite component (*S-UMTS*) that provides services to mobile users in different scenarios, such as: (i) back up coverage for areas already covered by terrestrial cellular systems; (ii) main system in regions for which the terrestrial coverage is unfeasible or not convenient. In such context, appealing UMTS services to be provided via broadband satellite are *High Speed Downlink Packet Access (HSDPA)* for point-to-point connections [1],[2] due to its high downlink data rate capacity, and *Multimedia Broadcast/Multicast Services (MBMS)* for point-to-multipoint connections [3], due to the wider coverage provided by the satellite. In both S-HSDPA and S-MBMS cases a *GEOstationary (GEO)* bent-pipe satellite is considered.

This paper investigates packet scheduling techniques for *Satellite HSDPA (S-HSDPA)* and provides some insights for traffic management in *Satellite MBMS (S-MBMS)*. Both services have been standardized by 3GPP for the terrestrial 3G scenario; however, such standards are not fully applicable to the satellite case. In particular, the specific satellite channel characteristics such as longer propagation delays, Doppler effects, atmospheric attenuation and multipath fading differ greatly from those commonly associated to terrestrial wireless systems. Moreover, the adoption in S-HSDPA of a direct satellite return link adds special requirements to the *User Equipment (UE)*.

For these reasons, a re-definition of both HSDPA and MBMS services architectures is required that meets the satellite environment and is still capable of providing *Quality of Service (QoS)* levels comparable to those achieved in the terrestrial case. In the case of HSDPA, the application of *Adaptive Coding and Modulation (ACM)* and multi-code operation dependent on the channel conditions experienced by the UE in the forward link, requires the exchange of channel state information between UE and the scheduler.

Due to the inherent longer propagation delays in the satellite scenario, the channel state information adopted by the scheduler is not up-to-date. Therefore, this paper investigates the adoption of ACM and scheduling in such demanding scenario.

In the S-MBMS case, this paper investigates an architecture without return link via satellite in order to simplify the implementation of UEs; the return link is provided via a terrestrial channel. Since there is no real-time interaction between the users and the satellite radio access network, the working of the packet scheduler is therefore different than that in the HSDPA case, where the packet scheduler can optimize its resource allocation based on its awareness of the channel state information from measurements provided by UEs.

In summary, this paper proposes S-HSDPA and S-MBMS architectures that meet the satellite environment and constraints. Moreover, it investigates scheduling issues for HSDPA by applying ACM on the basis of a non-accurate estimate of the channel state due to the round-trip delays.

This paper is organized as follows: Section 2 provides an overview of the terrestrial HSDPA architecture and proposes its evolution towards the satellite case; Section 3 discusses the design of the packet scheduler for S-HSDPA; Section 4 proposes a meaningful architecture for S-MBMS and discusses the design of the related packet scheduler; Section 5 describes the S-HSDPA results obtained with a simulator; finally, Section 6 draws some conclusions.

2. Packet Scheduling for Satellite-HSDPA

2.1 Evolution of terrestrial HSDPA towards S-HSDPA

The main targets of HSDPA are to increase user peak data rates (up to 10 Mbit/s), and to improve spectral efficiency for downlink asymmetrical and bursty packet data services, supporting mixture of diverse services with different QoS requirements [4]. In order to achieve this, the HSDPA concept is based on a time-shared channel [an evolution of the *Downlink Shared Channel* (DSCH) denoted as *High-Speed DSCH*, HS-DSCH] that supports a 2 ms *Transmission Time Interval* (TTI), fixed *Spreading Factor* (SF) of 16, no power control, ACM and fast physical layer hybrid ARQ. The shorter TTI compared to the WCDMA terrestrial air interface and the fact that the scheduling functionalities are located in the Node-B, allow for a fast adaptation to the channel state variations with a granularity of 1 TTI (= 2 ms). It is possible to increase the throughput provided to UEs with better channel conditions, even by multi-code transmission, i.e., assigning several spreading codes (up to 15 codes) to the same UE. If only one UE cannot fill the channel capacity during the TTI, more UEs can transmit in the same TTI, each of them using a different spreading code, thus optimizing the channel utilization. Moreover, the shorter TTIs in HSDPA allows for a faster channel adaptation and minimal wasted bandwidth. The adaptiveness of HS-DSCH to channel conditions is based on the code rate, the modulation scheme, and the number of codes applied. In particular, QPSK and 16QAM modulations are foreseen. By combining coding, modulation and multi-codes, the UE may receive theoretically up to 10 Mbit/s under very good channel conditions [4]. However, this might be constrained by the UE capabilities, due to the limitation of receiving several parallel codes [5].

According to a certain packet scheduling algorithm, the HS-DSCH transport channel is mapped onto a pool of physical channels, *High Speed Physical Downlink Shared Channels* (HS-PDSCHs), to be shared among all the HSDPA users in a time-multiplexed way. The means of adaptation are the code rate, the modulation scheme, the multi-codes operation. In particular, the HS-DSCH encoding scheme is based on the Release'99 rate-1/3 turbo encoding, but adds rate matching with puncturing and repetition to obtain a high resolution on the effective code rate, approximately from 1/6 to 1/1 [4]. To facilitate very high peak data rates, the HSDPA concept has added 16QAM on top of the existing QPSK scheme available in Release'99. A modulation and code combination is denoted as a *Transport Format and Resource Combination* (TFRC).

The packet scheduler can be considered as the central entity of the HSDPA design. In the HSDPA protocol stack architecture, the packet scheduler is located in the Node B, as a function of the HSDPA-specific MAC layer, called MAC-hs. The scheduler governs the distribution of the radio resources available in the cell among the UEs, i.e., it selects which UE is scheduled in the next TTI and supported by the link adaptation functionality, the TFRC and number of assigned codes. The scheduler relies on channel state information sent from each UE in order to perform its function. The UE is requested to regularly send a specific *Channel Quality Indicator* (CQI) on the uplink *High Speed Physical Control Channel* (HS-DPCCH); CQI provides the following information related to the transmission characteristics currently supported by the UE [6]:

- TFRC mode (modulation and coding used);
- Number of parallel codes that can be used by the UE for its transmission;
- Specification of a *transport block size* for which the UE would be able to receive at a value of *Frame Error Rate* (FER) $\leq 10\%$ (after first transmission).

There are different CQI tables for several UE categories. Table 1 shows an example of CQI values for some categories of HS-DSCH [7]. The *Radio Network Controller* (RNC) commands the UE to report the CQI with a certain periodicity from the set {2, 4, 8, 10, 20, 40, 80, 160} ms. If CQI indicates that the quality is degrading, the scheduler can choose a less ambitious ACM level, which will cope better with the poor conditions. As described in Appendix A, a GOOD/BAD channel model has been considered in our Satellite-HSDPA scenario.

Considering the discussion above, the terrestrial HSDPA architecture is not fully applicable to the satellite scenario. Firstly, the location of the different network entities, such as Node-B or RNC, is not uniquely determined in a satellite-based UMTS system. Depending on the available complexity on the satellite (with or without on-board processing), part of the functionalities typically located at the Node-B (e.g., packet scheduler) or at the RNC can be executed on board or not. Moreover, the fast adaptations to channel conditions are partially based on the proximity between UE and scheduling entity. The satellite scenario disables such fast adaptation capability, especially in the case that the scheduler is located on the earth, at the Gateway station.

In this paper, a multi-beam GEO bent-pipe satellite has been considered. All *Radio Access Network* (RAN) functionalities corresponding to the network part are located at the Gateway, as can be observed in Figure 1. It is assumed that the UEs in the domain of a specific Gateway remain in the coverage area managed by that Gateway. We investigate the applicability of ACM based on a feedback on the channel state (with delays due to the high round-trip time) and different scheduling options.

As can be observed in Figure 1, when a packet is transmitted by the Gateway (i.e., Node B) it takes approximately 280 ms to deliver the packet to the UE; then a channel estimation is performed and sent back (in the form of CQI) to the Gateway still with a delay of 280 ms. Hence, in our GOOD/BAD channel model case, 560 ms are spent from the channel variation to the instant when a packet with the appropriate TFRC is received. In such circumstances, an ACM scheme can only be employed if channel variations are sufficiently slow (as it is the case of shadowing phenomena in GEO satellite communications). During such large interval there is a misalignment between the channel state and the adopted transmission mode that allows an inefficient utilization of radio resources. For instance, if the channel makes a transition from GOOD to BAD, we have that for 560 ms packets (transport block) are transmitted with an inadequate (low) coding protection and are typically lost.

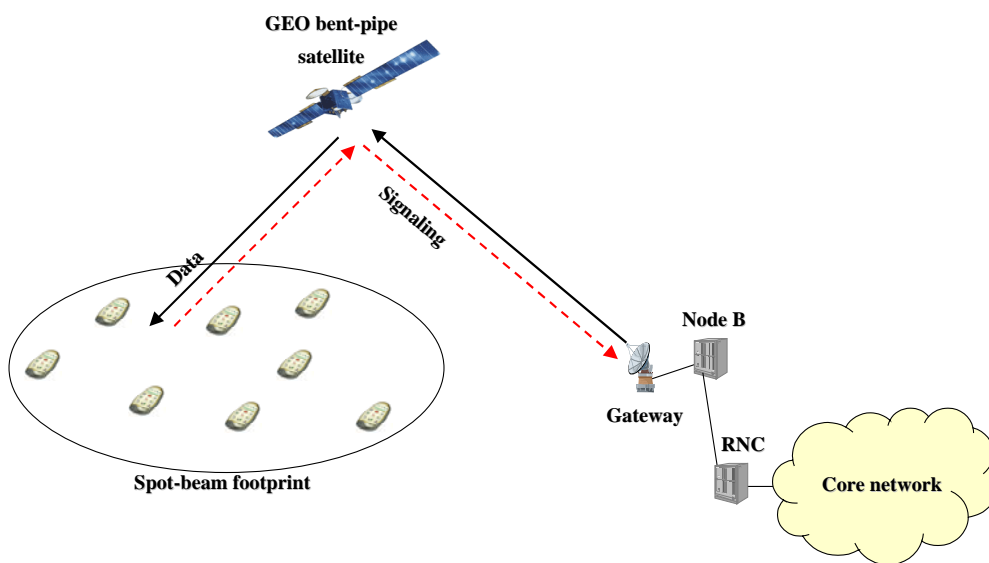


Figure 1: Functional architecture of S-HSDPA.

Since the CQI value is outdated at the arrival to the Gateway, delay compensation strategies shall be applied that predict what will be the channel evolution by the time that the CQI information is at the Gateway. The considerations of such predictions is out of the scope of this paper; however, for the interested readers some techniques as those proposed in [8] could be adapted. Once the time dynamics of the system is characterized, the next issue is what are the resources to be managed and how. In the case of HSDPA, there are several grades of freedom to be considered before each transmission occurs. Note that HSDPA has a sort of hybrid TDMA/CDMA air interface, where packet scheduling is done in two dimensions: time and code. By using the multi-code operation either the UE throughput can be improved on a TTI basis or several UEs can be allocated in the same TTI using different codes. However, the resource allocation task also depends on the CQI value allowed for each UE and that depends on the experienced channel conditions. Each UE shall estimate its instantaneous channel conditions, which might be different among UEs due to different locations and possibly different weather conditions in their respective locations. Then, each UE should map this information onto a certain CQI that the Node-B at the Gateway can identify.

Upon reception of such information, the Gateway (and in turn the scheduler) uses Table 1 to determine which is the most suitable modulation and coding pair to be applied at the physical layer, how many orthogonal codes are assigned to the UE and the transport block size (i.e., number of bits per TTI). With

Table 1. CQI mapping for TTI = 2 ms from the terrestrial standard; gray cases are those considered for our simulations referring to a GOOD/BAD channel model

CQI value	Mod. & coding	# Codes assigned per TTI	Bits per TTI (transport block size)
1	QPSK	1	137
2	1/3	1	173
3	(on each	1	233
4	code 960	1	317
5	bits are	1	377
6	sent in a	1	461
7	TTI)	2	650
8		2	792
9		2	931
10		3	1262
11		3	1483
12		3	1742
13		4	2279
14		4	2583
15		5	3319
16	16QAM	5	3565
17	1/3	5	4189
18	(on each	5	4664
19	code	5	5287
20	1920 bits	5	5887
21	are sent	5	6554
22	in a TTI)	5	7168
23		7	9719
24		8	11418
25		10	14411
26		12	17237
27		15	21754
28		15	23370
29		15	24222
30		15	25558

this information, the packet scheduler shall identify which is the best candidate UE to get service for the next TTI.

From Table 1 we can calculate the coding rate used for each case (i.e., CQI value), considering that a *Cyclic Redundancy Check* (CRC) code of 24 bits is added to each transport block and that the resulting bits are coded with rate 1/3 (with additional puncturing and repetition) to achieve a number of physical layer bits equal to:

- 960 bits × number of assigned codes in the QPSK mode;

- 1920 bits × number of assigned codes in the 16QAM mode

The effective coding rate is given by:

$$\text{Code rate}(CQI) = \frac{24 + (\text{transport block size})}{b_{code} \times (\text{number of codes})}$$

where $b_{code} = 960$ bits for QPSK modes and $b_{code} = 1920$ bits for 16QAM modes.

For the method used in HSDPA to pass from transport to physical layer an interested reader can refer to [9].

2.2 Design of a packet scheduler for S-HSDPA

The scheduler entity might establish priorities among the different existing flows for each TTI. On one hand, the criterion to improve channel efficiency leads to the decision to serve with maximum allowable throughput those UEs with better channel conditions (opportunistic scheduler). However, this approach does not guarantee an adequate service fairness among UEs, since those UEs with relatively bad channel conditions compared to others with better conditions, shall be blocked, whereas their channel state can be still good enough to transmit. A suitable trade-off

between opportunistic and fair scheduling shall be identified by combining them through a hybrid criterion, as envisaged in this paper. In addition to this, prioritization should also account for the urgency of the different traffic classes.

Efficient support of Internet-based applications is a key feature of 3G networks, as well as the support of multimedia applications. These services should be also provided via satellite. In the last years some projects like ATB (*Advanced S-UMTS Test Bed*), GAUSS (*Galileo And UMTS Synergetic System*) and SATIN (*SATellite UMTS IP-based Network*) have been developed to demonstrate the realistic feasibility of packet mode transmissions for S-UMTS [10],[11]. In these projects, as in this paper, the target scenario includes GEO satellites with multiple spot-beams.

Considering a GEO S-UMTS system, the maximum round-trip propagation delay of about 560 ms plays a crucial role in the design of the S-UMTS system, because the main distinguishing factor between the QoS classes is how delay sensitive the traffic is. Taking into account this great delay, it should be analyzed whether HSDPA-like transmissions with ACM on the basis of a feedback (CQI) are still convenient in the satellite scenario. In our study, we will keep the TTI value of terrestrial systems (= 2 ms) for a finer granularity in traffic scheduling, but we consider that the UEs provide CQI updates in larger time scales (such choice, permitting to save transmission power on UEs, is not that critical considering that the channel information is anyway outdated upon arrival at the Gateway). In particular, we have selected the CQI interval equal to 40 ms (¹). During the time interval between two CQI updates, channel conditions are considered constant by the scheduler for a given UE. Hence, to be on the safe side preventing from retransmissions, more robust modulation and coding schemes can be applied in the satellite case in comparison with terrestrial HSDPA (transmission modes and related CQI values must be selected to allow a much lower target FER value at the first transmission than in the terrestrial HSDPA).

According to our GOOD/BAD transmission modes, we consider to use respectively CQI values 15 and 25 in Table 1. We assume that with such choice the FER is negligible. Due to the significant round-trip propagation delay, there are time intervals (of 560 ms) during which the transmission is done with a CQI not appropriate for the channel. In particular, in the presence of a transition from BAD to GOOD, for 560 ms the system uses a more conservative mode than necessary and FER = 0. Whereas, in the presence of a transition from GOOD to BAD for 560 ms the system does not adequately protect transmission so that we assume to have FER = 1.

We consider serving one UE per TTI. The task of the scheduler is to select the UE to be served with the transmission of a transport block in the current TTI among all the active UEs. Once a UE is served, one transport block is transmitted in the TTI interval collecting all the IP packets available for this UE so as to fill in (in the best way) the block capacity². Two CQI values and corresponding transport block sizes are used depending on the fact that the scheduled UE has a channel in the GOOD or in the BAD state: 14411 bits (i.e., CQI = 25) and 3319 bits (i.e., CQI = 15), respectively. In general, the CQI value selection depends on channel characteristics, attenuation, antenna patterns, modulation and coding performance, interference conditions, UE position in the spot-beam; here, an arbitrary choice has been made. A further refinement is needed based on a realistic channel model.

If the traffic generated by the UE is not so high (and there are not congestion conditions) it may occur that when a transport block is assigned to the UE its IP packets available at the scheduling time partly fill in the block capacity (some capacity is unused). This problem may cause a non-optimal utilization of radio resources and, hence, a low efficiency.

¹ Depending on the CQI transmission timing with respect to the current state transmission from the UE channel state, the delay to receive a packet with an updated TFRC ranges from 560 to 600 ms.

² We consider here one UE for each traffic flow.

We describe below two alternative scheduling schemes: *Proportional Fairness* (PF) and *Earliest Deadline First* (EDF).

PF scheduler

In the terrestrial arena, some work has been done in order to find a suitable scheduling strategy that is able to track channel conditions and at the same time to provide fairness and QoS. In [4] and [12], comparative tables on the performance of different scheduling techniques are provided with the conclusion that the PF scheduler is the most suitable trade-off solution (in the case of a single traffic class). This strategy serves the UE with largest *Relative Channel Quality Indicator* (RCQI), which represents the ratio between the maximum data rate currently supported by each UE (according to its CQI and the corresponding transport block size; see Table 1) and the UE throughput averaged on a sliding window of suitable width. This approach allows a trade-off in the service between the UEs that have better channel conditions and those that up to now have received less resources. RCQI is evaluated as shown below [13]:

$$RCQI_k[n] = \frac{R_k[n]}{T_k[n]} \quad n = 1, 2, \dots \quad (2)$$

where k is the UE index and n is related to the time measured in TTI units. Moreover, $R_k[n]$ is the supported bit-rate in the next TTI (depending on its CQI) for the k -th UE; $T_k[n]$ represents the average throughput for the k -th UE obtained up to the present TTI.

$R_k[n]$ and $T_k[n]$ can be computed as follows [13]:

$$R_k[n] = \min \left\{ CQI_k[n], \frac{B_k[n]}{\text{TTI}} \right\} \quad (3)$$

$$T_k[n] = \left(1 - \{B_k[n] > 0\} \cdot \frac{1}{N_k} \right) \cdot T_k[n-1] + \frac{1}{N_k} \cdot R_k'[n-1] \quad (4)$$

where $CQI_k[n]$ is the maximum bit-rate supported by the k -th UE at the current time calculated as the throughput that is allowed by the CQI in the next TTI interval. In particular, referring to the adopted GOOD/BAD channel model (see Appendix A) with the selected ACM levels specified in Table 1, we have: $CQI_k[n] = R_{bad} = 3319$ bits/TTI ≈ 1.6 Mbit/s in the BAD state and $CQI_k[n] = R_{good} = 14411$ bits/TTI ≈ 7.2 Mbit/s in the GOOD state. Moreover, $B_k[n]$ represents the amount of data waiting for transmission in the Node-B buffer of the k -th UE at current time; $\{B_k[n] > 0\}$ is either 1 or 0 depending on whether the Boolean expression is right or not; N_k represents the memory of the averaging filter (set to 1000 TTI units in our case) and $R_k'[n-1]$ denotes the bit-rate used for the transmission to the UE during the $(n-1)$ -th scheduling interval. We have assumed $T_k[1] = CQI_k[1]$.

EDF scheduler

In this technique, packets are served according to their urgency: each packet has a deadline to be transmitted; the packet with the shortest residual life is transmitted. Such scheme requires the dynamic management of the buffer for each traffic class when we have to serve packets with different deadline

values. The EDF scheme is quite appropriate for the management of real-time traffics. EDF is well suited to manage packet data traffic with deadlines, as in the case of real-time traffic flows.

To implement the EDF criterion we have considered that the priority index for the generic k -th UE at the current n -th TTI interval, $P_k[n]$, is given by the ratio between the transmission delay of its oldest IP packet, $d_k[n]$, and the packet deadline, $T_{deadline}$:

$$P_k[n] = \frac{d_k[n]}{T_{deadline}} \quad n = 1, 2, \dots \quad (5)$$

The above priority index does not permit to prioritize the real-time video traffic with respect to the interactive Web traffic (i.e., the two traffic classes considered in this study for the S-HSDPA scenario). This approach could degrade the video performance especially in the presence of significant Web traffic load. To cope with this need, we have considered a differentiation in the priority index in (5). In particular, we use (5) for video traffic so that a video IP-packet has an increasing priority up to (almost) 1 when the packet is close to its deadline and risks to be dropped. Moreover, we use a modified priority index for Web IP-packets that saturates to 0.9 when these packets are close (or exceed) their virtual deadline (see the Appendix):

$$P_k[n] = \min \left\{ 0.9, \frac{d_k[n]}{T_{deadline}} \right\} \quad n = 1, 2, \dots \quad (6)$$

Hence, very urgent video packets will be served always with highest priority than any Web packet. In what follows, we will denote simply as EDF the scheme where the priority index (5) is used for both video and Web traffic flows; whereas, we name ‘Prioritized-EDF’ (P-EDF) the scheme where the priority index (5) is used for video and the priority index (6) is used for Web traffic flows.

3. Packet Scheduling for MBMS Traffic

With the expected increasing use of high bandwidth applications in 3G systems, especially with a large number of UEs receiving the same high data rate services, efficient information distribution is essential. Broadcast/multicast is a method for transmitting datagrams from a single source to several destinations. Thus, broadcast and multicast are techniques to decrease the amount of transmitted data within the network and to use resources more efficiently. This resource saving is made possible as the data is sent just once by the network and transmitted to UEs, located in the same cell, over a single common channel without clogging up the air interface with multiple transmissions of the same data by multiple unicast sessions. This efficient delivery technique is currently under standardization for the terrestrial 3G networks within the MBMS framework in 3GPP [14].

Due to their unique wide area coverage capabilities, satellites are a promising platform for MBMS delivery. In order to provide acceptable UE performance for the reception of broadcast and multicast services, the allocation of resources to these services in downlink must be carefully managed. This is where packet scheduling plays a pivotal role in assigning for each time instant radio resources to individual flows of services based on a particular policy.

3.1 Impact of broadcast and multicast services delivery requirements on packet scheduler design

Similar to the 3G network, S-MBMS is envisaged as a *Content Delivery Network*, primarily oriented towards *streaming* (e.g., audio/video broadcasting) and download applications (e.g., infotainment, entertainment, software delivery). These streaming and download services are mapped onto the streaming and background UMTS QoS classes, respectively. Notably, the classification of applications under the two service delivery modes, i.e., streaming and download, is not strict. In fact, all non-real time services may be provided in both modes. The mechanism for the service delivery to a particular group is determined by other factors including UE capabilities, policies, and timing context of service.

With streaming services, the multimedia content is played directly upon reception at the UE from a playout buffer. With streaming video or streaming media, a UE does not have to wait to download a large file before seeing the video or hearing the audio. Instead, the media is sent in a continuous stream and is played as it arrives. On the other hand with download services, the multimedia content is stored locally in a cache for later processing (pre-stored content), and therefore, they are also normally known as push & store applications. It is envisaged for S-MBMS that the download services can be further classified into two types: ‘hot download’ and ‘cold download’; the difference between the two is that the former is sensitive to delay. The types of applications belonging to this hot download service may include broadcasting of urgent/important messages, such as emergency announcements, and monitoring of variable data, such as stock exchange data. The QoS profile showing the *Radio Access Bearer* (RAB) service attributes for streaming and download traffic classes over S-MBMS can be found in [3]. The packet scheduler needs to take into consideration the different QoS requirements of the two MBMS traffic classes (i.e., delay and target error rate) in its resource allocation and scheduling policy.

Besides meeting the QoS requirements of the video/audio streaming and file downloading applications, there are still many challenging issues to be solved in order to provide an efficient use of radio resources. One of the main challenging tasks in the QoS management is the support of the QoS constraints with the same conditions for all the members belonging to a multicast group. Moreover, since the number of members in a multicast session can be dynamically changing, there may be a need for RAB reconfiguration, and hence there should be a criteria for when the RAB re-assignment will be necessary, which will certainly affect the scheduling assignment. Another issue to consider is on the method the transmission power should be (re)assigned to reflect the group dynamics of a multicast session, since UEs can join or leave a multicast group at any time. Since the transmission power has impacts on the performance of the connection, such as contribution to the total interference level and the corresponding error behavior, controlling the transmission power is crucial in maximizing the capacity that the network is capable of supporting.

3.2 Impact of S-MBMS architecture on packet scheduler design

Considering that broadcast and multicast traffics are asymmetric in nature, the baseline satellite system architecture under consideration is effectively unidirectional [15], as illustrated in Figure 2. It relies on the existing 3G mobile network point-to-point (p-t-p) service capability for the return link to manage and control the services delivered, for example for access to content decoding keys and retrieval of multimedia content blocks corrupted on the satellite forward link.

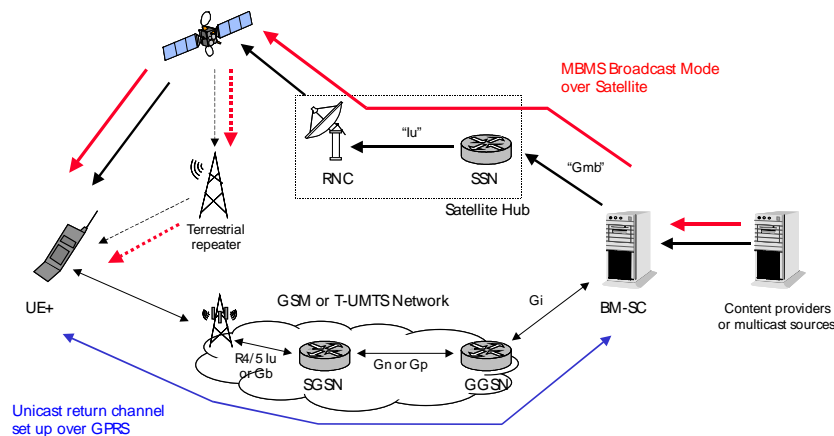


Figure 2: S-MBMS architecture and its interworking with a terrestrial segment.

The UE is a multi-mode terminal (i.e., satellite and terrestrial 2G/3G radio access enabled), with frequency band extension. It is able to perform parallel idle mode, i.e., maintaining either GSM activity or UMTS activity during S-MBMS reception. The basic type does not have a dedicated receiver for SDMB and is then required to switch from UMTS terrestrial to satellite reception. The space segment consists of a GEO satellite that features a transparent payload with multiple beams. This choice provides the desired flexibility in updating/enhancing the system throughout its life and is accompanied by reduced technology and investment risk. In build-up areas such as in the urban and indoor environments, terrestrial repeaters/gap-fillers are introduced to enhance the signal availability and are designed to be smoothly co-sited with the 3G base station to prevent additional installation costs [11]. The hub includes 3G RAN equipment (i.e., RNC) and 3G core network functions. It collects incoming media services from the *Broadcast-Multicast Service Center* (BM-SC) and generates the W-CDMA waveform and redirects signal to the satellite feeder link. The BM-SC provides functions for S-MBMS UE service provisioning and delivery, for example, it controls UE access to services, authorizes and initiates bearer services within the network, and schedules and transmits MBMS data across the network.

Given that there is no real-time interaction between the UE and the satellite RAN in the considered baseline architecture, the working of the packet scheduler is therefore different than in the previous HSDPA case [16]. The packet scheduler in the unidirectional satellite system will have to decide on allocations without knowledge of the state of individual channels, i.e., channel state dependent scheduling is not possible. In any cases, even if such information were available, it would have to be exploited in a complex manner due to the point-to-multipoint nature of the services, i.e., the decisions regarding the scheduling of a single service data flow need to consider the state of multiple links corresponding to all the UEs that have activated the service in each (multicast) group.

3.3 Design of a packet scheduler for S-MBMS

The role of the packet scheduler in S-MBMS is not that dominant in determining the system throughput as it is the case in the T-UMTS [2]. Nevertheless, the scheduler is still responsible for two important tasks that are executed with a period equal to the TTI of the radio bearers [17].

- Time multiplexing of flows with different QoS requirements into fixed physical channels, in a way that can satisfy these requirements.
- Adjusting the transmit power of the physical channel carrying the data flows on the basis of the required reception quality of the service (in terms of the target BLER)³ under the constraint that the total available power for all the physical channels within a beam is fixed.

Herein the framework for packet scheduling for S-MBMS is described. The packet scheduling strategy can be generally conceptualized into two steps, as described in Figure 3.

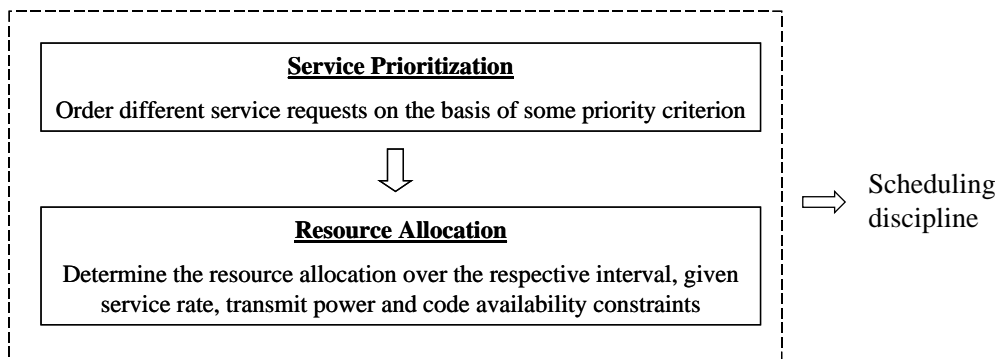


Figure 3: S-MBMS packet scheduling procedure.

These two steps effectively constitute the scheduling discipline of the packet scheduler; they differentiate one from another and define the capability of each one to integrate the service QoS requirements with an efficient system resource utilization.

Service prioritization

In MBMS, each service is mapped one-to-one onto an *MBMS point-to-multipoint Traffic CHannel* (MTCH) logical channel, which is then mapped onto the *Forward Access Channel* (FACH) transport channel. At the physical level, the *Secondary Common Control Physical CHannel* (S-CCPCHs) can carry one or more FACH(s) [18]. The incoming service requests are ordered according to some priority criterion. In selecting the respective criteria, the service attributes are considered, which are normally mapped onto the traffic handling priorities as defined by the UMTS QoS classes. Note that the prioritization can be more or less dynamic; in a more dynamic prioritization, the relative priority of the different channels may change in each resource allocation interval (this is normally the TTI), depending for example on the maximum delay tolerated by a service or the number of packets buffered, as compared to a more static approach.

Resource allocation

Once all the services to be transmitted are prioritized, the next step is the allocation of resources to them, which consists of bit-rate and transmit power assignments within the specific resource allocation interval (i.e., TTI). The data rate assignment consists of the selection of the *Transport Format Combinations*

³ This is for the case of *static rate matching*; when dynamic rate matching is employed, the transport block size to be served needs to be considered in the power allocation decision as well.

(TFCs), which directly determines the per FACH transport block size. For each active physical channel (S-CCPCH), the exact TFC is selected from the *Transport Format Combination Set* (TFCS), which is passed during the admission of a new service and its mapping on a specific bearer. This TFC selection step is of paramount importance since the capacity allocated to each service is strongly related to the QoS perceived by the end users, and, therefore, the selection of the TFC has to take into consideration constraints in terms of service requirements (e.g., minimum guaranteed rate, maximum tolerated delay) as well as system-level constraints (system load, transmit power per beam).

As for the power allocation, the transmit power setting for the S-CCPCH is based on the required reception quality of the active service flows mapped to S-CCPCH, which in our case is defined in terms of the most demanding target BLER among these service flows. The calculated power is only allocated as long as it is within the constraint of the total available power for all the physical channels, which is fixed within a beam. As can be seen, in the resource allocation step, the per S-CCPCH TFC selection and power allocation happen in parallel.

4. S-HSDPA Simulation Results

In order to study the performance of S-HSDPA transmissions, we have implemented a simulator that generates traffic at the IP level considering different traffic classes and schedules it on the S-HSDPA resources. Our simulator supports video and Web traffic sources in the presence of a GOOD/BAD channel model, as detailed in Appendix A. We assume that data from only one UE is scheduled in one TTI, i.e., multi-code operation refers to the allocation of one or more codes to one UE.

We introduce below the performance metrics that will be used in our simulations:

- i. Percentage of IP-video packets lost due to deadline expiration, P_{drop} ;
- ii. Mean delay for the transmission of an IP Web packet, $Delay_{Web}$;
- iii. Efficiency in the utilization of radio resources, η ;
- iv. Percentage of IP packets lost due to GOOD-to-BAD channel misalignment, $P_{loss_channel}$ (note that in this preliminary study we have not considered the retransmission of lost packets).

Let C denote the mean capacity considering the GOOD/BAD channel model described in Appendix A and the related CQI values associations in Table 1. Hence, the resource utilization efficiency η (< 1) can be measured as follows:

$$\eta = \frac{\text{Mean aggregated transmitted bit - rate}}{C} . \quad (7)$$

P_{drop} is obtained as the ratio between the number of IP-video packets that are lost due to deadline (= 150 ms) expiration and the number of generated IP-video packets. $P_{loss_channel}$ is computed as the ratio of the number of IP packets (considering video and Web traffic together) that are lost at the receiver due to the GOOD-to-BAD channel misalignment and the number of transmitted IP packets. Finally, parameter $Delay_{Web}$ is computed as the ratio between the sum of the transmission delay experienced by Web packets and the total number of generated Web packets.

In the following graphs, the above different performance metrics are plotted as a function of the *system load*, ζ , that is defined as:

$$\zeta = \frac{\text{Mean aggregated generated bit - rate}}{C} \quad [\text{Erl}] . \quad (8)$$

Of course, $\eta \leq \zeta$ due to the fact that not all the generated bits are transmitted (some of them may be dropped due to deadline expiration in the case of video traffic).

The following simulation results have been obtained considering an equal number of video and Web traffic sources (we will refer to the total number of traffic sources as the sum of both video and Web ones); video and Web sources produce the same mean bit-rate according to the formulas detailed in Appendix A.2. Each simulation run corresponds to 4×10^4 s. Three scheduling techniques are compared: PF, EDF and P-EDF.

Figure 4 shows the P_{drop} behavior as a function of ζ for PF, EDF and P-EDF for cases with total number of traffic sources equal to 30. All these scheduling schemes employ the physical layer adaptability, but PF and EDF achieve extremely poor P_{drop} performance since they do not include a strategy to provide a strong prioritization of video traffic with respect to the Web one. Whereas, P-EDF attains a low P_{drop} value that permits to fulfill the P_{drop} requirement ($\leq 1\%$) up to ζ about equal to 1 Erl.

Figure 5 shows the $Delay_{Web}$ behavior as a function of ζ for PF, EDF and P-EDF for cases with total number of traffic flows equal to 30. As expected EDF and PF schemes allows the lowest $Delay_{Web}$ values; the high $Delay_{Web}$ values with the P-EDF scheme is due to the strong prioritization of video traffic that entails higher transmission delays for the Web traffic.

In the following graphs, we will restrict our interest to P-EDF and PF techniques. Figure 6 presents the comparison of the achieved η as a function of ζ for PF and P-EDF for cases with total number of traffic flows equal to 30. We can note that P-EDF allows a better efficiency than PF since it permits to achieve a lower P_{drop} value.

Finally, Figure 7 provides $P_{loss_channel}$ results as a function of ζ for PF and P-EDF for cases with total number of traffic flows equal to 30. The obtained results show that all the $P_{loss_channel}$ values are quite close and around 7% ⁽⁴⁾. Even if this is a non-negligible loss probability value, it could represent an acceptable performance degradation due to the peculiarities of the satellite scenario.

Note that the PF scheduler in some way may provide a more frequent service to UEs in the GOOD state than P-EDF. Hence, with PF, it could be more probable to schedule a UE that is changing its state from GOOD to BAD (thus incurring in packet losses). Consequently, the more the number of UEs, the higher the probability that to schedule a user when a transition occurs from GOOD to BAD.

⁴ Note that if we would measure the P_{loss} in terms of transport block loss rate, we should have that it is upper bounded by the channel misalignment probability evaluated as $0.6 \text{ s} / 8 \text{ s} = 0.075$.

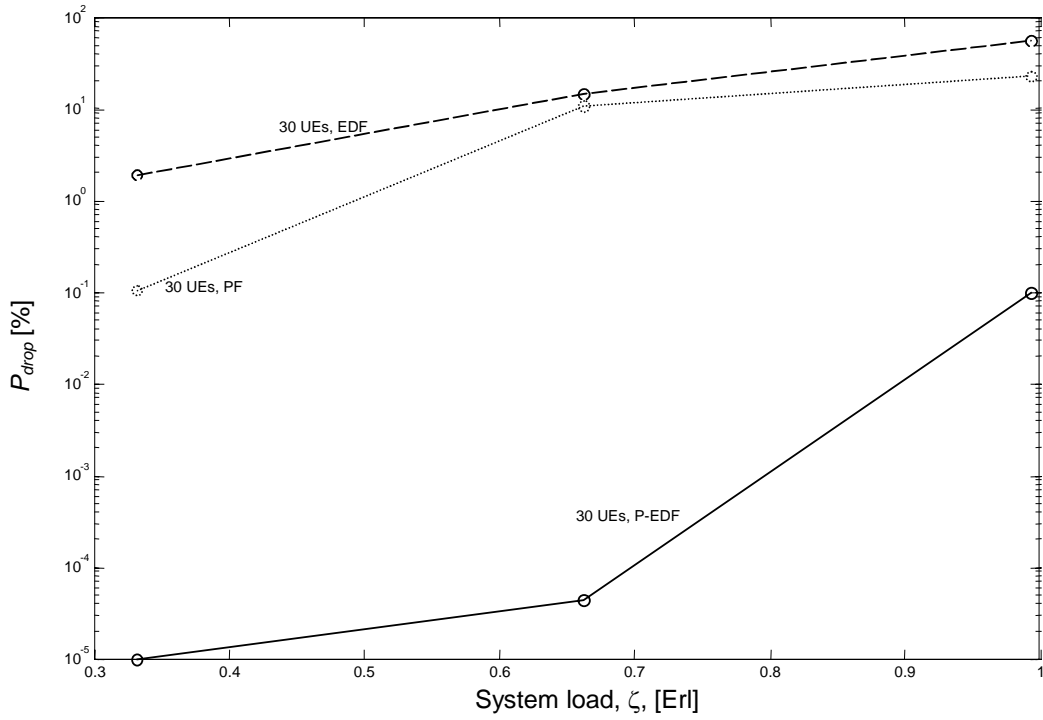


Figure 4: S-HSDPA results in terms of P_{drop} for video IP-packets.

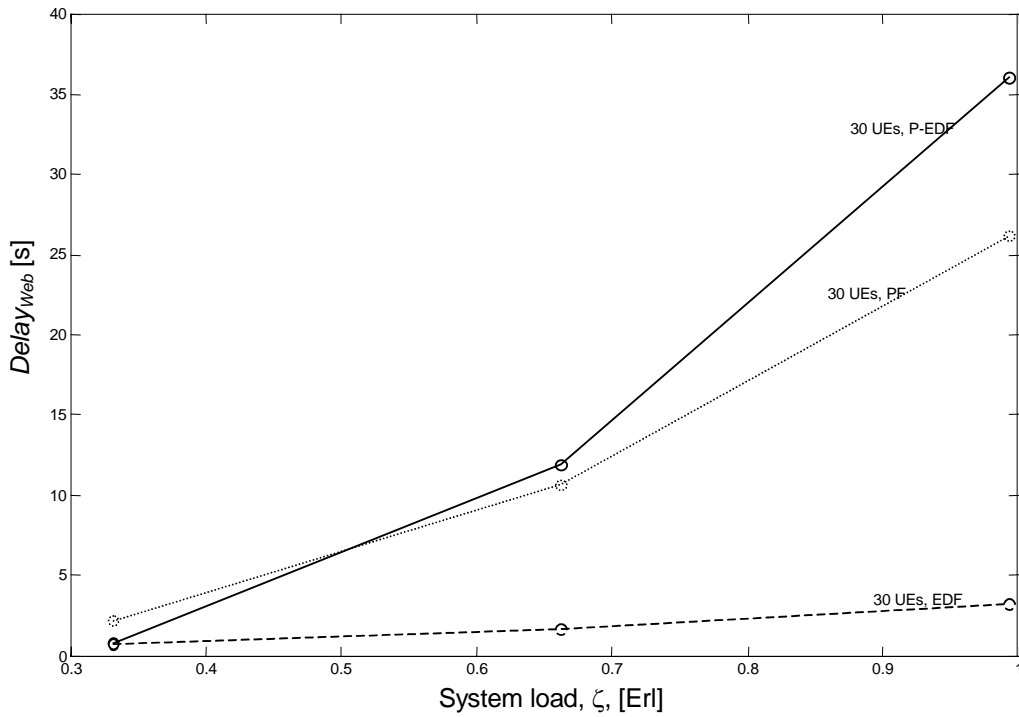


Figure 5: S-HSDPA results in terms of $Delay_{Web}$ for Web IP-packets.

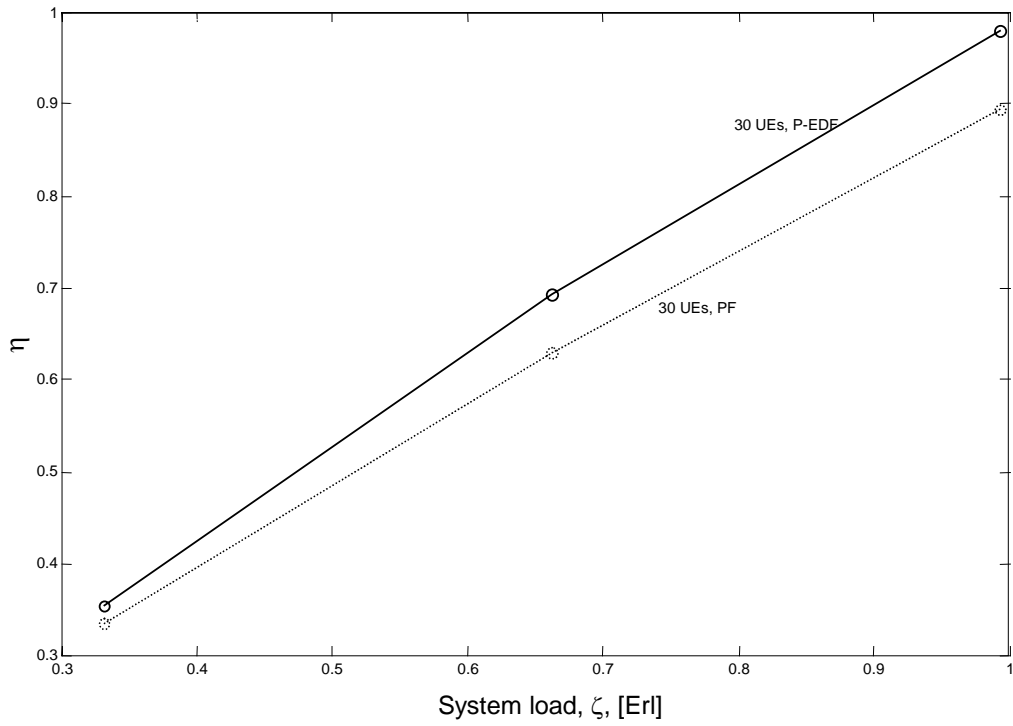


Figure 6: Resource utilization efficiency comparison as a function of system load for P-EDF and PF schemes.

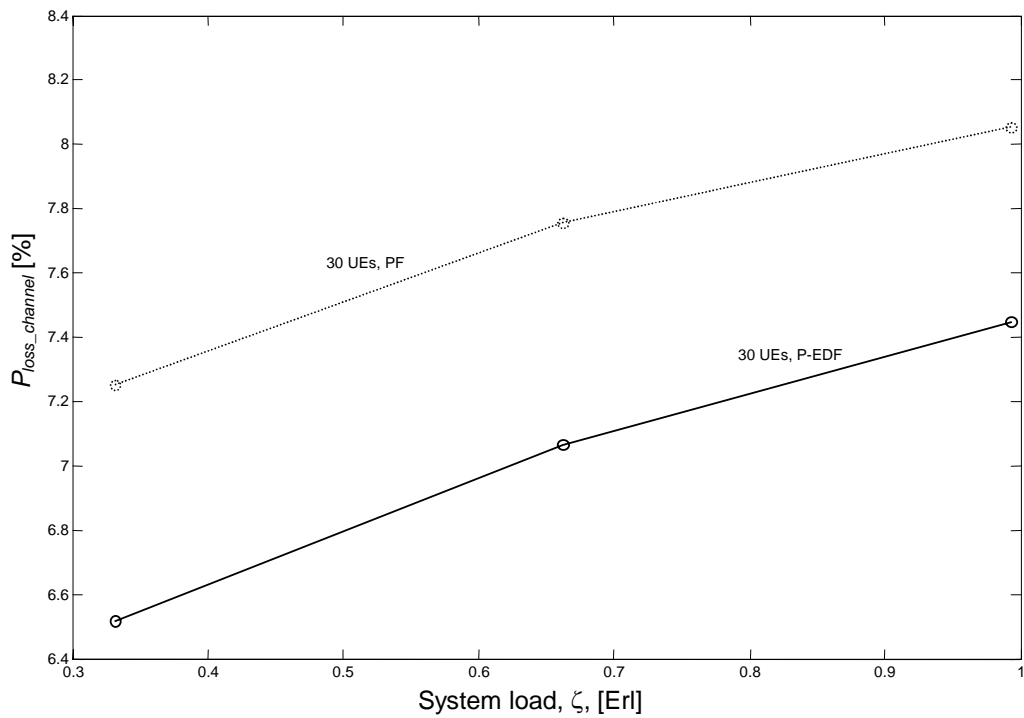


Figure 7: $P_{loss_channel}$ as a function of system load for P-EDF and PF schemes.

5. Conclusions

Satellite communications have a potential market in providing high downlink bit-rate services and in supporting multicast services on broad areas of the earth. For this reasons, this paper has focused on HSDPA and MBMS provision via a GEO bent-pipe satellite. In both cases suitable network architectures and radio resource management techniques have been investigated to support such services in an appropriate and efficient way. The preliminary simulation results shown in this paper prove that S-HSDPA is feasible, provided that suitable scheduling functions and traffic flow prioritization are employed. A further investigation is needed to improve the PF scheduler to account for differentiated traffic classes.

Appendix

This Section provides details on the adopted models for the radio channel (GEO case) and for generating multimedia downlink traffic.

A.1 Adopted channel model

The blocks (packets) received by the UEs from the satellite are subject to errors according to a GOOD-BAD channel model [19]. The GOOD state is related to unshadowed periods (LOS path and multipath); the BAD state is related to shadowed propagation conditions (only non-LOS paths). Sojourn times in GOOD and BAD states are exponentially distributed. The mean sojourn time in the GOOD and BAD states, T_{good} and T_{bad} , depend on the UE speed and the traveled distances in LOS and non-LOS conditions. Let us refer to the channel characterization made in [19] for the GEO MARECS satellite that transmits in the L band; these data can be acceptable also for the band at 2 GHz for 3G mobile satellite systems. In particular, referring to a highway scenario (a scenario that is well suited for GEO satellite communications) with 13° of elevation angle, we have that the mean traveled distance in the GOOD state (BAD state) is 90 m (29 m). Thus, assuming a user speed of 60 km/h, $T_{good} = 6$ s and $T_{bad} = 2$ s.

Due to the high round-trip delay of satellite communications of about 560 ms (GEO bent-pipe case) it is possible that the satellite transmits (based on the CQI measure at the time t) the AMC level for the GOOD state, whereas the channel becomes BAD at the time $t_1 (= t + 560$ ms) when the UE receives the packet. In such a case, we consider that the transport block is completely lost (i.e., FER = 1). In the opposite case (i.e., transmission with AMC for the BAD state and reception in the GOOD one), we neglect the occurrence of packet errors. Finally, for the transmissions in GOOD (BAD) state with reception of the packet in the GOOD (BAD) state, we consider a negligible FER after FEC decoding.

On the basis of the transport block size values we use in our scenario (see Table 1), we want to calculate the system capacity C under the assumption that we schedule one UE per TTI interval. Let P_{bad} (P_{good}) denote the probability of the BAD (GOOD) state. We have:

$$P_{bad} = \frac{T_{bad}}{T_{bad} + T_{good}} = 0.25 \quad \text{and} \quad P_{good} = \frac{T_{good}}{T_{bad} + T_{good}} = 0.75 . \quad (9)$$

Let R_{bad} (R_{good}) denote the bit-rate corresponding to the CQI and related transmission mode selected for a TTI interval in the BAD (GOOD) state. We have already shown that for our numeric assumptions we have: $R_{bad} = 1.6$ Mbit/s and $R_{good} = 7.2$ Mbit/s. Correspondingly, we have the following expression for the capacity C :

$$C = R_{bad} P_{bad} + R_{good} P_{good} \approx 5.8 \quad [\text{Mbit/s}]. \quad (10)$$

A.2 Adopted traffic models

Video traffic model

Each video source has been modelled as a *Discrete-time Markovian Arrival Process* (D-MAP) [20]. The bit-rate produced by a video source has been considered as the aggregated output of M independent minisources, each alternating between OFF and ON states. Each minisource in the ON state produces traffic at the constant rate of A bit/s; whereas in the OFF state no traffic is generated. Time is considered to evolve in discrete steps, called slots, which last one TTI ($= 2$ ms) interval. The time interval (in slots) spent in ON and OFF states are geometrically distributed with parameters $\alpha = 1/p$ and $\beta = 1/q$, where p and q are the mean times spent in ON and OFF in slots, respectively. A minisource in the ON (or OFF) state makes a transition towards the OFF (or ON) state, at the end of a slot with a probability α (or probability β). We have considered that in a slot at most one minisource can make a transition from ON to OFF or vice versa. Hence, there are not sudden traffic variations for a video source. Parameters p , q and A of a minisource are generated by the formulas below:

$$A = \frac{\mu}{M} + \frac{\sigma^2}{\mu} \left[\frac{\text{bit}}{\text{s}} \right], \quad q = \frac{1}{a \times \text{TTI}} \left(1 + \frac{M\sigma^2}{\mu^2} \right) [\text{TTI units}], \quad p = \frac{1}{a \times \text{TTI}} \left(1 + \frac{\mu^2}{M\sigma^2} \right) [\text{TTI units}] \quad (11)$$

where μ is the mean bit-rate, σ^2 is the variance of the bit-rate and parameter a characterises the slope of the auto covariance function of the bit-rate produced by the video source. We have assumed: $M = 10$ and $a = 3.9 \text{ s}^{-1}$. Moreover, on the basis of some data in the literature, we have added the further condition to relate μ and σ parameters for video traffic:

$$\mu/\sigma = 16. \quad (12)$$

By using the above M and a values and (12) in the q and p formulas in (11), we obtain: $p = 3410.253$ [TTI units] and $q = 133.213$ [TTI units]. Then, by using (12) and the A formula in (11) we have: $A = \mu/10 + \mu/256 \approx 0.104\mu$. Hence, the mean bit-rate produced by a video source is proportional to the mean bit-rate produced by an ON minisource. We have varied the μ parameter to vary the system load.

The b bits generated by the above video source in 20 ms form a video frame that is sent as an IP packet by adding 4 bytes for the *Real-time Transport Protocol* (RTP) and 20 bytes of the IP header. Hence, the resulting IP packet has a (variable) length L_v , characterised as follows:

$$L_v = (b + 4 + 20) \times 8 \quad [\text{bits}] \quad . \quad (13)$$

Such IP packet length L_v cannot exceed the *Maximum Transfer Unit* (MTU) that is here assumed equal to 1500 bytes. If L_v is greater than 1500 bytes more than one IP packet is needed to convey a video frame.

For the video IP-packets we have considered a deadline $T_{deadline}$ of 150 ms: if a video packet is not transmitted within 150 ms it is dropped, thus contributing to P_{drop} . For an acceptable video quality we consider $P_{drop} \leq 1\%$.

Web downloading traffic model

Referring to a given Web session, a Web source alternates between a *packet call state* during which segments are downloaded and a *reading time state* where no traffic is produced. This is a simplified model derived from [21]. The number of segments per packet call is geometrically distributed with expected value $m_{Nd} = 300$. The segment interarrival time and the reading time are exponentially distributed with mean values m_{Dd} (this is a variable parameter that is used to change the mean bit-rate and the burstiness of the traffic produced by this source) and $m_{Dpc} = 2$ s, respectively. The activity factor for this source is $\psi_w = m_{Nd} m_{Dd} / (m_{Nd} m_{Dd} + m_{Dpc})$. Each segment has a random length in bytes $l_{byte} = \lfloor x \rfloor$, where symbol $\lfloor \cdot \rfloor$ denotes the *floor function* and x is a random variable with the following truncated Pareto *probability density function* (pdf) with parameters $\nu = 1.1$, $k = 815$ bytes and $m = 664$ kbytes:

$$pdf(x) = \frac{\nu k^\nu}{x^{\nu+1}} [u(x-k) - u(x-m)] + \left(\frac{k}{m}\right)^\nu \delta(x-m) \quad (14)$$

where $u(\cdot)$ is the unitary step function and $\delta(\cdot)$ is the Dirac delta function.

It is easy to show that each Web traffic source proposed here produces a *two-state Markov Modulated Poisson arrival Process* (2-MMPP) of segments.

The mean bit-rate generated by this Web source, γ , can be evaluated as follows:

$$\gamma = \frac{8\psi_w E[l_{byte}]}{m_{Dd}} \left[\frac{\text{bit}}{\text{s}} \right] \quad (15)$$

where $E[l_{byte}] = \frac{\nu k - m \left(\frac{k}{m}\right)^\nu}{\nu - 1} \approx 4796$ is the mean segment length in bytes.

Let us consider that $m_{Nd} m_{Dd} \gg m_{Dpc}$ (i.e., $m_{Dd} \gg 150^{-1}$ s). Hence, $\psi_w \approx 1$ and $\gamma \approx \frac{8 \times 4796}{m_{Dd}}$. Therefore,

the mean bit-rate generated by a Web source is proportional to $1/m_{Dd}$. Hence, we have varied the m_{Dd} parameter to vary the system load.

Each segment of length l_{byte} receives a 40-byte header due to the TCP/IP protocols. Hence, datagrams have a length L_w as:

$$L_w = (l_{byte} + 40) \times 8 \quad [\text{bits}] \quad . \quad (16)$$

If such datagram length exceeds the MTU value of 1500 bytes, the datagram is fragmented in more IP packets.

In the case of the EDF scheduler, we consider a 'virtual' deadline $T_{deadline}$ of 2 s for IP packets produced by the Web source. This deadline is virtual in the sense that if an IP packet is not transmitted in time, it is not discarded, but it is still transmitted.

Acknowledgments

This paper has been funded by the "SatNEx" NoE project (contract No. 507052) under the 6th framework of the European Commission - joint activity 2430 (QoS&RRM).

References

- [1] 3GPP, "High Speed Downlink Packet Access; Overall UTRAN Description", TR 25.855, Release 5.
- [2] H. Holma, A. Toskala, *WCDMA for UMTS: Radio Access for Third Generation Mobile Communications*. Second edition, John Wiley & Sons Ltd, 2002.
- [3] 3GPP, "Multimedia Broadcast/Multicast Service; Architecture and Functional Description", TS 23.246, Release 6.
- [4] T. E. Kolding, K. I. Pedersen, J. Wigard, F. Frederiksen, P. E. Mogensen, "High Speed Downlink Packet Access: WCDMA Evolution", *IEEE Vehicular Technology Society News*, Vol. 50, No. 1, pp. 4-10, February 2003.
- [5] H. Ishii, A. Hanaki, Y. Imamura, S. Tanaka, M. Usuda, T. Nakamura, "Effects of UE Capabilities on High Speed Downlink Packet Access in WCDMA Systems", in *Proc. of the 59th Vehicular Technology Conference VTC2004-Spring*, Milan May 17-19, 2004.
- [6] 3GPP, "Physical layer procedure (FDD)", TS 25.214 v6.3.0 (2004-09).
- [7] 3GPP, "UE Radio Access capabilities", TS 25.306 v6.2.0 (2004-06).
- [8] C. Párraga, C. Kissling, "Delay Compensation Strategies for an Efficient Radio Resource Management in DVB-S2 Systems," in *Proc. of the International Workshop of Satellite and Space Communications, IWSSC'05*, September 8-9, 2005, Siena, Italy.
- [9] 3GPP, "User Equipment (UE) Radio Transmission and Reception (FDD)", TS 25.101, Release 6.
- [10] K. Narenthiran, *et al.*, "S-UMTS access network for MBMS service delivery: the SATIN approach", *International Journal of Satellite Communications and Networking*, January-February 2004.

- [11] T. Severijns, *et al.*, "The Intermediate Module Concept within the SATIN Proposal for the S-UMTS Air Interface", in *Proc. of the IST Mobile Summit 2002*, Greece.
- [12] L. Wang, M. Chen, "Comparisons of Link Adaptation Based Scheduling Algorithms for the WCDMA System with High Speed Downlink Packet Access", *Canadian Journal of Electrical and Computer Engineering (CJECE)*, Vol. 29, No. 1/2, pp. 109-116, January/April 2004.
- [13] T. Kolding, "Link and System Performances Aspects of Proportional Fair Scheduling in WCDMA/HSDPA", in *Proc. of the IEEE VTC-Fall 2003*, 4-9 October, Orlando, Florida, USA.
- [14] V. Y. H. Kueh, M. Karaliopoulos, B. G. Evans, "Service Characterization and Traffic Mix Derivation for Satellite Digital Multimedia Broadcast (SDMB) System", in *Proc. of the 23rd AIAA International Communications Satellite Systems Conference (ICSSC 2005)*, Rome, Italy, 25-28 September 2005.
- [15] Draft ETSI (2004-09): "Satellite Earth Stations and Systems (SES); Satellite Component of UMTS/IMT-2000; Multimedia Broadcast/Multicast (MBMS); Inter-working with Terrestrial UMTS networks".
- [16] R. Ferrus, L. Alonso, A. Umbert, X. Reves, J. Perez-Romero, F. Casadevall, "Cross-layer Scheduling Strategy for UMTS Downlink Enhancement", *IEEE Communications Magazine*, Vol. 43, Issue 6, June 2005, pp. 24 - S28.
- [17] M. Karaliopoulos, P. Henrio, E. Angelou, B. G. Evans, "Packet Scheduling for the Delivery of Multicast/Broadcast Services via S-UMTS", in *Proc. of the First International Conference on Advanced Satellite Mobile Systems*, Frascati, Italy, July 2003.
- [18] 3GPP, "Introduction of the Multimedia Broadcast/Multicast Service (MBMS) in the Radio Access Network; Stage 2 (Release 6)", TS 25.346 V6.3.0, December 2004.
- [19] E. Lutz, D. Cygan, M. Dippold, F. Dolainsky, W. Papke, "The Land Mobile Satellite Communication and Recording, statistics and Channel Model", *IEEE Trans. Veh. Tech.*, Vol. 40, pp.375-386, May 1991.
- [20] B. Maglaris, D. Anastasious, "Performance Models of Statistical Multiplexing in Packet Video Communications", *IEEE Transactions on Communications*, Vol. 36, No. 7, pp. 834-843, July 1988.
- [21] A. E. Brand, A. H. Aghvami, "Multidimensional PRMA with Prioritized Bayesian Broadcast - a MAC Strategy for Multiservice Traffic over UMTS", *IEEE Trans. on Veh. Tech.*, Vol. 47, No. 4, pp. 1148-1161, November 1998.